



PRIMARY RESEARCH

Localization of redundant robotic systems with wheeled mobile base: Theory and experiment

Behnam Pour Pir Ali ¹, Yaser Maddahi ^{2*}¹ Department of Computer Science, University of Manitoba, Winnipeg, Manitoba, Canada² Department of Research and Development, Tactile Robotics, Winnipeg, Manitoba, Canada

Keywords

Localization
Calibration
Linear regression
Sensory system
Localization
Mobile robots
Kinematics

Abstract

This paper presents a technique to reduce positional errors in redundant Wheeled Mobile Robots (WMRs) with omnidirectional wheels. The errors could originate from different resources during the process of design to fabrication of a WMR including modelling inaccuracy, backlash/joint deflection, and misalignment. The technique is explained based on the kinematic equations of WMRs, and could potentially be used to correct both the lateral and longitudinal errors observed during the movement of a non-holonomic mobile robot. The major advantages of this method are simplicity, time efficiency, and use of simple-to-understand kinematics equations. In addition, it uses the linear regression method – that is easy to use – to quantify the contribution of each wheel on observed errors. The effectiveness of the method was investigated by testing a prototype three-wheeled omnidirectional robot. According to the test results, the movements of the tested robot was improved, and the systematic errors decreased by at least 74%.

Received: 18 February 2019**Accepted:** 20 March 2019**Published:** 20 April 2019

© 2019 The Author(s). Published by TAF Publishing.

I. INTRODUCTION

WMR can be found in many applications such as in transportation, planetary exploration, and surveillance operations. Different forms and structures of wheels are used in WMRs including an omnidirectional mechanism that enables the robot to move in multiple directions without the installation of any caster wheels. The use of omnidirectional robots is particularly interesting because it implies that the omnidirectional mobile robots' mechanisms can be controlled with a reduced number of actuators, and are highly maneuverable in narrow or crowded areas such as residences, offices, and hospitals.

Positional errors during the movement of WMRs are inevitable to occur and should be rectified to ensure that the robot's performance is acceptable. Developing effective techniques to reduce positional inaccuracy has been interested in robotic systems [1, 2]. The techniques include odometry, 3D camera error detection, active beacons, gy-

roscope and magnetic compasses [3, 4, 5, 6, 7]. Odometry uses the information of positional sensors such as encoders attached to each actuator to estimate the change in position over time. The odometry method is applied to reduce the positional inaccuracy of different WMRs [4].

Some researchers have designed and manufactured different types of mobile robots and in some cases, the laboratory tests are discussed [8, 7, 9, 10]. [11] introduced a method for measuring odometry errors in differential drive mobile robots and by expressing these errors quantitatively. A method was introduced to develop an integrated system for mobile robot odometry relying on an existing wireless transceiver infrastructure [12]. The authors have previously proposed an odometry-based technique to reduce positional inaccuracy in WMRs with the differential drive or omnidirectional mechanism [13, 14, 15]. The technique provides short-term accuracy with high sampling rates and rectifies two lateral and longitudinal corrective factors. This

*Corresponding author: Yaser Maddahi

†email: ymaddahi@TactileRobotics.ca

technique uses the linear regression to model the relationship between the position error and the angular velocities of the two wheels, considering the physical and deterministic properties of the robot's components including the optical encoders attached to each wheel, without obtaining the precision associated with each estimate. Niola et al. present the problem of the camera system modelling and an algorithm for the calibration of the vision system [16]. This algorithm is suitable to be used to apply a vision model to robotic applications.

In this paper, the method proposed in [4] is mathematically simplified to be understandable by engineers and researchers, and be used in a simpler manner. The method is explained using the kinematic equations of the followed by showing test results. Moreover, the experimental tests on mobile robots demonstrating the systematic errors are done using the proposed method. Then, using this method, systematic errors of a prototype omnidirectional mobile robots are corrected and the robot movement is corrected. Finally, some pre-defined statistical indices are calculated in order to determine how efficient the calibration results are using this approach.

II. PROTOTYPE MOBILE ROBOTS

The shape and dimension of the main body of a mobile robot are specified by some input parameters during the design process. Several kinds of wheels can be attached to the wheeled mobile robot, depending on the design, selection, and wheel arrangement. The wheels fall into one of two categories: driving wheels and caster wheels. The driving wheels are actively rotated to permit the robot to move and the caster wheels merely ease the movement of the robot and enable its body to be suspended when no torque is applied to the axles. By replacing drive or caster wheels with omnidirectional ones, the number of wheels attached to the robot is reduced and the mobility of a robot is increased. Moreover, the mechanical characteristics of the robot would be completely altered. That is, the robot would be able to move and balance its body with only omnidirectional wheels.

This robot is designed with high maneuverability to move automatically from specific positions in an environment to desired points. The electromechanical configuration is composed of three drive wheels, a transmission system, a DC motor, and an electrical board. The omnidirectional wheels are centred on the longitudinal axis of the robot. These wheels are driven, and un-steering wheels powered by three completely independent mechanisms (see Figure 1 and Table 1).

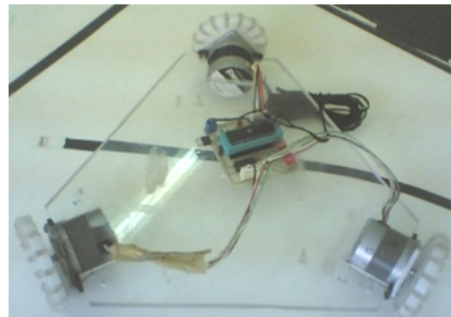


Fig. 1. Prototype omnidirectional mobile robot

TABLE 1
SPECIFICATIONS OF THE PROTOTYPE

Characteristic	Value
Dimension ($L \times W \times H$) (cm)	29x29x12
Weight (Kg)	1.150
Stall torques of motors (Nm)	0.2
Maximum speed (m/min)	3.65
Wheel radius (m)	0.07
Wheelbase (m)	0.16
Encoder resolution, (pulse/rev)	36

III. TEST ASSUMPTIONS

The essential assumption to derive the required calibration formulations is that an omnidirectional robot behaves as a differential drive robot in some situations. This supposition is that when the robot moves in a straight line, only two of the wheels have angular velocity and the motors of the third wheels have no rotation and behave as caster wheels. This means that in this condition the robot acts as a differential drive robot and we can use the formulations of differential drive robots. Figure 2 depicts the scenarios under which a three-wheeled robot operates as a differential drive robot. As shown in this figure, the first and second wheels move by V_1 and V_2 velocities. These velocity vectors have two components along the X and Y axes. When the robot travels in a straight path ($V_1 = V_2$), the difference between velocity components in x axis (V_{1x} and V_{2x}) creates the lateral error and the difference between velocity components along x direction (V_{1y} and V_{2y}) causes the longitudinal error. Considering the above assumptions, a benchmark method is proposed and all manufactured robots are tested in defined paths that satisfy this assumption. The classes related to three-wheeled and four-wheeled omnidirectional mobile robots and their motion properties are summarized in Table 1. As shown in this table, for three-wheeled robots, four trajectories (k_{12} , k_{13} , k_{23} and k_{123}) are predefined to implement the calibration. Also, seven different paths are considered for testing the four-wheeled robot including a rotation (k_{1234}) and six straight paths (k_{12} , k_{13} , k_{14} , k_{23} , k_{24} and k_{34}).

Since the main goal of this research is the implementation of a new approach to correct the systematic errors of omnidirectional mobile robots, the following section describes the kinematic modelling of differential drive robots.

IV. KINEMATICS MODELING OF MOBILE ROBOTS

In order to control the trajectory and then derive the needed calibration formula of a robot, the kinematics formulation is required to specify how the actuators and center of base variables affect the positioning of the robot.

The kinematic diagram of a planar omnidirectional mobile robot is shown in Figure 3. Each wheel is assumed to rotate independently and without slippage. The kinematics equations of differential drive-wheeled robots are used, and then based on these equations, independent non-holonomic constraints due to instant no-slip wheel conditions can be written as follows [16]:

$$\dot{x} \cos \theta + \dot{y} \sin \theta = 0.5(\dot{\varphi}_L + \dot{\varphi}_R) \tag{1}$$

$$\theta = r/2l (\varphi_R - \varphi_L) \tag{2}$$

$$\dot{x} \sin \theta = \dot{y} \cos \theta \tag{3}$$

Where, l indicates the distance from the center of gravity of the robot to the center of the wheels along a radial path, and XY is the coordination of the fixed world frame. θ represents the orientation of the robot with respect to the fixed

world frame, r is the radius of the wheels, and V'_R and V'_L are the slippage velocities of omnidirectional drive wheels. The parameters are shown in Figure 3. As described before, this figure notes that the omnidirectional wheels can be replaced by simple drive wheels; also, that omnidirectional robots can be replaced by differential drive robots in some trajectories.

TABLE 2
IMPLEMENTED TRAJECTORIES EXPERIMENTAL TESTS

Path	Class Motion Schematic
k_{12}	1 and 2 (D) 3 (C)
k_{13}	1 and 3 (D) 2 (C)
k_{23}	2 and 3 (D) 1 (C)
k_{123}	1,2 and 3 (D)

-D: Drive Wheel
-C: Caster Wheel
- K_{ij} : State which i th and j th wheel have rotation and the other wheels are considered as caster wheels.
- The arrows show the direction of robot motion

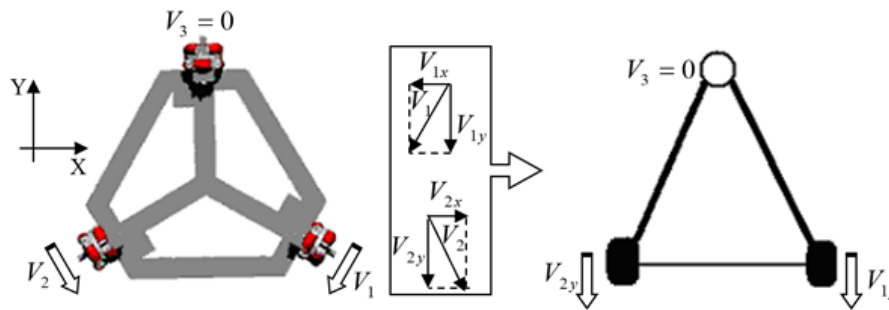


Fig. 2. The three-wheeled omnidirectional robot operates as a differential drive robot in particular situations

V. TEST PROCEDURE

In a typical indoor environment with a flat floor plan, localization becomes a matter of determining the position and orientation, collectively known as the state of the robot on a two-dimensional floor plan. Here, a new approach is used for the measurement and correction of systematic errors of wheeled mobile robots. Systematic errors include control and mechanical factors created while robot parts are designed, fabricated or assembled. The non-systematic group of errors is independent of the robot and has its own charac-

teristics. In other words, they are unwanted errors created during the robot's motion. If unexpected phenomena are ignored, the most important factor that affects the movement of a robot is the slippage that occurs between the wheels and the surface that the robot moves on. Table 2 shows a classification of a robot's errors including systematic and non-systematic errors.

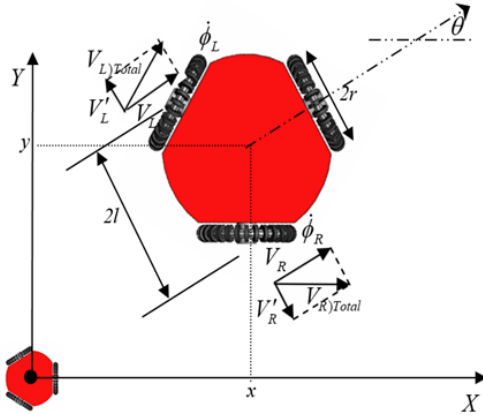


Fig. 3. Reference coordinate systems of a three-wheeled omnidirectional mobile robot

A. Correction Method

The new approach explained below is usable for all non-holonomic mobile robots. This methodology is based on the

derived equations in Section III and is used to correct the robot’s systematic errors. Also, this method improves the two types of robot errors called “Lateral Error” and “Longitudinal Error”.

B. Forward Straight Test

Using this method, the robot is programmed to travel along a straight line for n times, and the maximum offset of the final position from the desired Cartesian coordinate (XOY) is recorded. In this motion, only two of the wheels have rotation (drive wheels), and the motors of the other wheels are turned off. Figure 6 shows the designed trajectory and related variables of the proposed method.

Since all robots are equipped with encoders, the relationship between the pulse of the encoder and the angular revolution of each type can be expressed as follows:

TABLE 3
ERROR CLASSIFICATION IN WMRS

	Category	Sources
Systematic	- Control factors	Software factors: lack of pulse and/or an error in the pulse.
	- Mechanical factors	Hardware factors: changing or omitting the output pulses or not counting them properly. Repeated permanent errors: caused by non-circularity of the wheels, misalignment of the shafts and unequal wheel diameters, the difference between the averages of actual diameters with nominal wheel diameter and between the actual wheelbase with a nominal wheelbase, misalignment of wheels, finite encoder resolution, and sampling rate. Temporary errors: caused by all the types of backlash e.g. by means of the backlash between the gears or to the shafts not being radially fixed relative to their bearing.
Non-Systematic	- Travel over uneven floors	Slippery floors
	-Travel over unexpected objects on the floor	Over acceleration
	- Wheel slippage Fast turning External and internal forces Non-point wheel contact the floor	

$$\theta = \frac{N}{E} \times 2\pi \tag{4}$$

where E is the resolution of the encoder and varies for each type and N is the read pulse from the encoders.

According to Figure 4, the robot travels on the actual path instead of travelling on the desired path, due to the structural errors in the mobile robot. For correcting the systematic errors and then the robot’s motion, a rotation equal to -λ angle should be applied about the central axis of robot during its motion in order to compensate the created errors. Using Equation 2, the relationship between the new required angular velocities of the wheels (θ and θ’) should

be applied to the motors in order to reorient the robot to a straight path and approach the amount of λ to zero. The deviation angle (λ) is obtained using Equation 5.

$$\lambda = -\frac{r}{2l} (\theta - \theta') \tag{5}$$

In this equation, θ’ is the angular velocity of the faster wheel during the travel along the straight path.

The position is expressed with respect to the coordinate system attached to the desired endpoint (O). It means that all positions should be considered with respect to the XOY coordinate system.

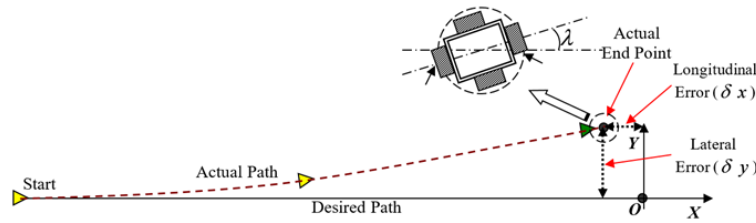


Fig. 4. The robot is programmed to move along a straight trajectory

To be clear, we define the lateral corrective factor (F_{lat}) for calculating needed angular velocities to correct the robot movement trajectory. This parameter is obtained by dividing two new angular velocities Equation 6.

$$F_{lat} = \frac{\theta'}{\theta} \tag{6}$$

Since $\theta' \geq \theta$, then $F_{lat} \geq 1$.

Figure 5 illustrates the notion of lateral and longitudinal errors in this method pictorially. Combining (4) to (6) con-

cludes the final formula.

$$F_{lat} = 1 + \frac{El\lambda}{rN\pi} \tag{7}$$

In Equation (7), λ is obtained from the results of experimental tests and N_N represents the initial input angular rotation (θ). Using Equation (7), the lateral corrective factor (F_{lat}) is calculated and then substituted into Equation (6), and finally, the amount of the new required rotation of the second wheel (θ') is calculated. The process is flow charted in Figure 6.

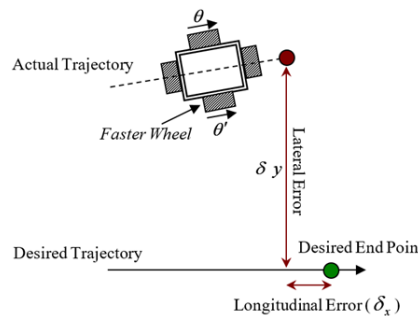


Fig. 5. Concepts of errors defined in the test method

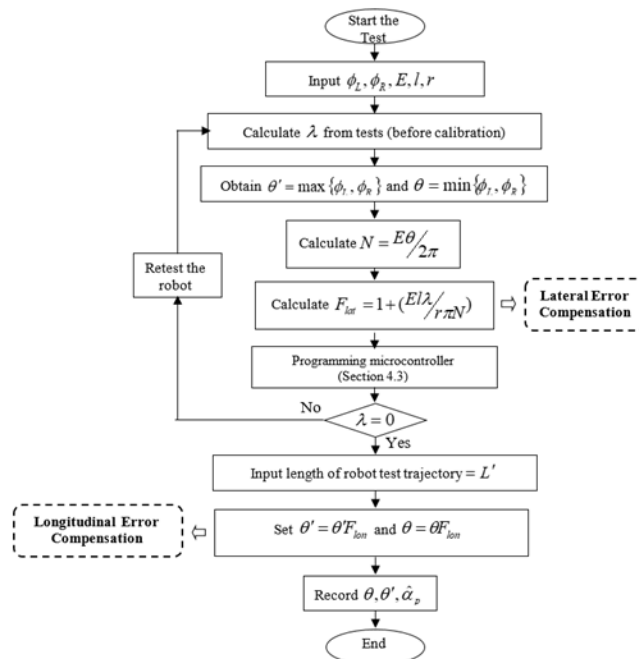


Fig. 6. Proposed test algorithm

Also, we understand that the amount of θ' differs with the initial amount of angular rotation of the right wheels before calibration (θ_R). This difference investigates that the systematic errors can be corrected by altering the amount of second wheel rotation from θ_R to θ' . According to the proposed procedure, the angular deviation λ converges to zero (the desired endpoint), and the robot travels on the desired path instead of the actual path as shown in the test results. Also, if the robot has longitudinal errors, this error can be modified by the multiplication of both θ and θ' to $F_{lon} = (L/L')$ coefficient, where L' is the length of the trajectory obtained from experimental tests before calibration (actual trajectory) and F_{lat} represents the longitudinal corrective factor.

C. Rotation Tests

In the next test, the robot is programmed to rotate about the central axis by 90° . As shown in Figure 7, the robot is placed in the actual position (solid line) instead of the desired one (dashed line). Thus, we should apply some coefficient to correct the robot motion. As shown in Figure 7, the three-wheeled robot (case study) stops in O_c instead of O_R . There are also three deviations, which include two longitudinal deviations (x_c and y_c) and one orientation deviation (θ_c), which should be compensated for by using the redundancy constraints. To reduce the above errors, the robot should be programmed to stop at point $(-x_c, -y_c)$ instead of $O_R (0,0)$, and rotate by $90-\theta_c$ instead of 90 . Then we need some partial amounts of angular rotation/velocity

($\varphi_{1c}, \varphi_{2c}$ and φ_{3c}) to apply to the motors as input velocities. Also, the new orientations are $90-\varphi_{1c}, 90-\varphi_{2c}$ and $90-\varphi_{3c}$, instead of 90 degrees for all motors.

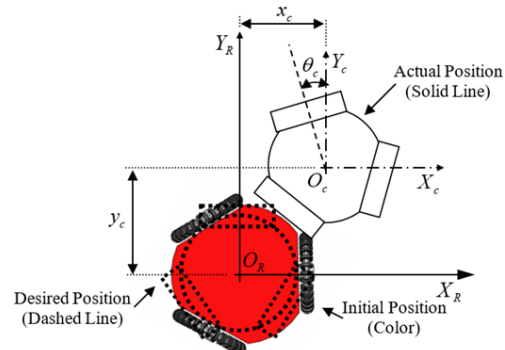


Fig. 7. The desired and actual position of the robot in rotation along its central axis

To calculate the amount of error for each robot, we need to find the relation between the angular velocities of the wheels and the posture of the robot. This relation can be expressed using the no-slip constraint equations as follows:

$$R\phi \cos \gamma - x \cos (\theta + \alpha_i) - y \sin (\theta + \alpha_i) - r_i \phi_i = 0 \quad (8)$$

where i is the number of wheels and α_i is the angle between the i th motor shaft and x-axis.

Considering the initial position of the three-wheeled robot shown in Figure 5, the Jacobian matrix can be obtained, and the number of rotational errors is calculated using the following expression:

$$\begin{Bmatrix} \dot{\varphi}_{1c} \\ \dot{\varphi}_{2c} \\ \dot{\varphi}_{3c} \end{Bmatrix} = \frac{1}{l} \begin{bmatrix} \sin (-\theta_c) & \cos (-\theta_c) & r \\ \sin (-\theta_c + 2\pi/3) & \cos (-\theta_c + 2\pi/3) & r \\ \sin (-\theta_c + 4\pi/3) & \cos (-\theta_c + 4\pi/3) & r \end{bmatrix} \begin{Bmatrix} -\dot{x}_c \\ -\dot{y}_c \\ -\dot{\theta}_c \end{Bmatrix} \quad (9)$$

Having the Jacobian Matrix for each case, the amount of $\varphi_{1c}, \varphi_{2c}$ and φ_{3c} are calculated and the created errors can be reduced by applying the new angular rotation to robot inputs.

As demonstrated, the importance of our proposed method is using the kinematics equations of a robot, which are simple to understand, and using them with respect to other existing methods. In fact, a geometrical definition describing the relationship between motor variables and robot parameters is defined as the basic formulation of this test. Also, this method is very simple to implement and doesn't need complicated initializing before starting.

VI. EXPERIMENTAL RESULTS

This section presents the results of introduced experimental tests applied to described omnidirectional mobile robots after and before testing, separately. Also, some statistical indices are defined and applied to conclude data in order to verify the test results in both methods. For comparison between robot operations before and after calibrations, and for a better understanding of the position of the robots in each trial, the radial position (δr) and the mean error improvement (δr_m) are defined as follows:

$$\delta r = \sqrt{(\delta x)^2 + (\delta y)^2} \quad (10)$$

$$\delta r_m = \left[\frac{r_{cg, before} - r_{cg, after}}{r_{cg, before}} \right] \times 100 \quad (11)$$

where δX and δY are defined in Figure 5. One of the most important probability distributions, from both the theoretical and practical viewpoint, is the Gaussian distribution (or as mathematicians call it, the normal distribution). The distribution diagram of data derived from experimental tests is important to predict the future behaviour of robots in motion. Also, when the data cover the normal distribution criteria, it means that they obey regular rules and validate the results obtained from experimental tests. Another advantage of the normal distribution is the logical prediction of future behaviour of robots in the same trajectories. In fact, when the obtained data follow the normality conditions, the future response of robot (motion) can be predicted. To cover the normality conditions, the amount of Std. Error of Skewness and Std. Error of Kurtosis should be between -2 and 2. Using SPSS software, Std. Error of Skewness and Std. Error of Kurtosis variables are calculated based on data derived from experimental tests in radial direction.

As will be shown in the next section, the resulting radial errors for all tested paths are varied and follow the Gaussian distribution criteria. The basic formulation for Gaussian distributions in the radial direction is defined as

$$p(r_{cg}) = \frac{1}{\sqrt{2\pi}\sigma} e^{-\left(\frac{r_{cg}-\mu}{2\sigma^2}\right)} \quad (12)$$

TABLE 4
STATISTICAL INDICES OBTAINED FROM EXPERIMENTAL TESTS

	k_{12}		k_{13}		k_{23}		k_{123}	
	Before	After	Before	After	Before	After	Before	After
Max Error	43.26	11.31	34.05	10	37.80	10	18.44	2.23
Min Error	36.87	5.65	27.65	4.47	33.60	6.08	12.80	1
Mean Error	40.35	8.40	30.78	7.81	35.74	8.23	15.32	1.61
Std. Error of Kurtosis	-1.28	-0.47	-0.26	-0.81	-0.74	-1.23	-1.31	-1.97
Std. Error of Skewness	-0.53	0.41	-0.11	-0.51	-0.08	-0.47	0.33	-0.05

VII. DISCUSSION

Results obtained from experimental tests using the proposed method showed that the method is effective to reduce systematic errors. As shown, for the prototype robot, the minimum value of mean error improvement factors are calculated at 74.63%. These data confirm the effectiveness of this method in order to reduce systematic errors. As shown in Table III, the Std. Error of Skewness and the Std. Error of Kurtosis of the robot were between -2 and 2. These values showed that the derived data satisfy the normal distributions criteria that indicate that future motions of the robot

where μ is the average radial error and σ represents the standard deviation of each test group. Figure 8 depicts the coordinates of obtained data for a three-wheeled robot in after state and before state calibration conditions. The number of trials (n) for these tests is considered equal to 10. As shown in this figure, k_{ij} means the i th and j th wheels of the robot have equal and opposite angular rotations and other motors are turned off. Also, the minimum, maximum, average, Std. Error of Kurtosis, and Std. Error of Skewness parameters are shown in Table 2.

As shown in Table 4, the mean error improvements (δr_m) for k_{12} , k_{13} , k_{23} and k_{123} tests obtained are 79.18%, 74.63%, 76.97% and 89.49%, respectively. It can be seen that this method has been efficient in decreasing the systematic errors for this robot.

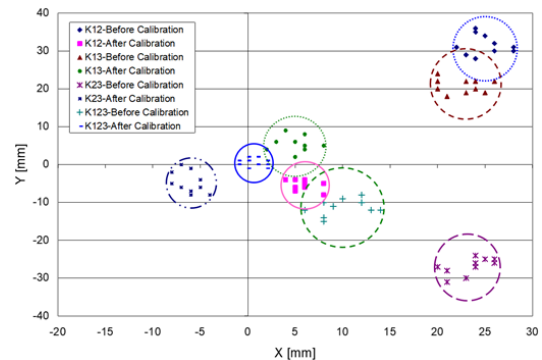


Fig. 8. Final positions of the prototype robot in the defined paths

are most probably predictable.

VIII. CONCLUSION

A method was proposed to reduce positional errors in omnidirectional mobile robots. A prototype omnidirectional mobile robot was tested with a focus on correcting systematic errors. A brief explanation of the prototype robot was presented followed by formulating required equations for the proposed test algorithm. Also, to overcome the systematic errors, a new benchmark method was proposed based on the derived kinematic equations. Then, the robot was

tested and moved in some pre-defined trajectories defined in the proposed method. Results showed that the systematic errors were significantly reduced using the proposed method in the tested robot. Finally, the absolute measurements of errors were compared to the desired position and

orientation of the robot. All experimental data satisfied the criteria of the normal distribution that showed that the results would be possibly repeatable in future tests. As a new work, the non-systematic errors can be obtained considering some supposed obstacles in laboratory test plates.

REFERENCES

- [1] J. An and J. Lee, "Robust positioning and navigation of a mobile robot in an urban environment using a motion estimator," *Robotica*, vol. 37, no. 8, pp. 1320-1331, 2019. doi: <https://doi.org/10.1017/s0263574718001534>
- [2] M. Vulic, M. Pavlovic, D. Tadic, A. Aleksic, and A. Tomovic, "Ranking of recycling technologies metal components of end of life vehicles by using modified electre," *Journal of Advances in Technology and Engineering Studies*, vol. 4, no. 4, pp. 143-148, 2018. doi: <https://doi.org/10.20474/jater-4.4.1>
- [3] M. B. Moldwin and L. V. Ojeda, "Magnetic beacon and inertial sensor localization technology," 2019. [Online]. Available: <https://bit.ly/2QDvrQU>
- [4] Y. Maddahi, A. Maddahi, and N. Sepehri, "Calibration of omnidirectional wheeled mobile robots: Method and experiments," *Robotica*, vol. 31, no. 6, pp. 969-980, 2013. doi: <https://doi.org/10.1017/s0263574713000210>
- [5] M. Piaggio, A. Sgorbissa, and R. Zaccaria, "Navigation and localization for service mobile robots based on active beacons," *Systems Science*, vol. 27, no. 4, pp. 71-83, 2001. doi: <https://doi.org/10.1109/iros.2001.976370>
- [6] F. Lamiroux and J.-P. Lammond, "Smooth motion planning for car-like vehicles," *IEEE Transactions on Robotics and Automation*, vol. 17, no. 4, pp. 498-501, 2001. doi: <https://doi.org/10.1109/70.954762>
- [7] D. Nistér, O. Naroditsky, and J. Bergen, "Visual odometry for ground vehicle applications," *Journal of Field Robotics*, vol. 23, no. 1, pp. 3-20, 2006. doi: <https://doi.org/10.1002/rob.20103>
- [8] S. A. Rahok and O. Koichi, "Odometry correction with localization based on landmarkless magnetic map for navigation system of indoor mobile robot," in *4th International Conference on Autonomous Robots and Agents*, Los Angeles, LA, 2009.
- [9] X. Song and Y. Wang, "A novel model-based method for odometry calculation of all-terrain mobile robots," in *7th World Congress on Intelligent Control and Automation*, New Dehli, India, 2008.
- [10] K. Punaiyah and H. Singh, "Biped robot for walking and turning motion using raspberry Pi and Arduino," *International Journal of Technology and Engineering Studies*, vol. 3, no. 2, pp. 49-58, 2017. doi: <https://doi.org/10.20469/ijtes.3.40002-2>
- [11] J. Borenstein and L. Feng, "Measurement and correction of systematic odometry errors in mobile robots," *IEEE Transactions on Robotics and Automation*, vol. 12, no. 6, pp. 869-880, 1996. doi: <https://doi.org/10.1109/70.544770>
- [12] P. Marantos, Y. Koveos, J. Stergiopoulos, A. Panousopoulou, and A. Tzes, "Mobile robot odometry relying on data fusion from RF and ultrasound measurements in a wireless sensor framework," in *16th Mediterranean Conference on Control and Automation*, New York, NY, 2008.
- [13] Y. Maddahi and A. Maddahi, "Mobile robot experimental analysis based on kinematics," *WSEAS Transactions on Circuits and Systems*, vol. 3, no. 8, pp. 1662-1667, 2004. doi: <https://doi.org/10.1017/s0263574713000210>
- [14] Y. Maddahi, N. Sepehri, A. Maddahi, and M. Abdolmohammadi, "Calibration of wheeled mobile robots with differential drive mechanisms: An experimental approach," *Robotica*, vol. 30, no. 6, pp. 1029-1039, 2012. doi: <https://doi.org/10.1017/s0263574711001329>
- [15] Y. Maddahi, M. Seddigh, M. M. Pour, and M. Maleki, "Simulation study and laboratory results of two-wheeled mobile robot," *WSEAS Transactions on Systems*, vol. 3, no. 9, pp. 2807-2812, 2004. doi: <https://doi.org/10.1017/s0263574713000210>
- [16] V. Niola, C. Rossi, and S. Savino, "Modelling and calibration of a camera for robot trajectories recording," in *Proceedings of 5th WSEAS International Conference on Signal Processing, Robotics and Automation*, Istanbul, Turkey, 2006.